Mechanisms of size-dependent shape evolution of one-dimensional nanostructure growth

Bing Wang, Yuhua Yang, Ningsheng Xu, and Guowei Yang*
State Key Laboratory of Optoelectronic Materials and Technologies, Institute of Optoelectronic and Functional Composite Materials, School of Physics Science & Engineering, Zhongshan University, Guangzhou 510275, China
(Received 14 December 2005; revised manuscript received 7 November 2006; published 4 December 2006)

The size-dependent morphological evolution of one-dimensional (1D) SnO_2 nanostructures has been observed in experiment. It was found that the shape formations of nanowire and nanobelt of SnO_2 are size dependent, i.e., the wire is favorable when the size is less than 90 nm and the belt is favorable when the size more than 90 nm, respectively, indicating that a critical size exists in the growth of SnO_2 nanostructures to determine their morphologies. The nucleation thermodynamics, growth kinetics, and morphological transition thermodynamics were established to elucidate the size-dependent morphological evolution. The theoretical predictions are consistent with experiments, suggesting that the thermodynamic driving force seems to be the physical origin of the shape evolution.

DOI: 10.1103/PhysRevB.74.235305 PACS number(s): 68.65.La

One-dimensional (1D) nanostructures such as wires, rods, belts, and tubes have become the focus of intensive research owing to their unique applications in mesoscopis physics and fabrication of nanoscaled devices. They not only provide a good system to study the electrical and thermal transport in one-dimensional confinement, but also are expected to play an important role in both interconnection and functional units in fabricating electronic, optoelectronic, and magnetic storage devices with nanoscale dimension.[1] It is well known that SnO_2 is an important functional material, which has been widely applied in the field of opto- and microelectronics. For instance, SnO_2 can be utilized in solar cells,[2] transparent conducting electrodes,[3] gas sensors,[4,5] and transistors.[6] In recent years, the assembly and synthesis of 1D SnO_2 nanostructures such as wires[7] and belts[8–10] have attracted great interest due to their unique applications in gas sensors and field-effect transistors. Therefore, to attain various nanometer sized building blocks, a lot of self-assembly and synthesis processes have emerged in recent years.[11] Importantly, these assembly and synthesis at the nanometer scale have revealed many unusual thermodynamic and kinetic behaviors of the microphase growth,[12–19] which plays an important role in the development of the classical thermodynamics.[20] Basically, self-assembly processes require atomic or clustering interactions as the thermodynamic driving force to organize those atoms or clusters to form nanosized domain morphologies.[21] For instance, Bartelt *et al.* recently reported the self-assembly of the regular arrays of two-dimensional (2D)-vacancy islands via absorbate-driven dislocation reactions.[22] Therefore, it is essential to pursue the physical and chemical origin causing the nanostructure to control the growth. On the other hand, the surface shape of 1D nanostructures plays a particular important role in their application. For instance, nanowires as wraparound gate transistors or core-shell heterostructures require good control of the surface shape to achieve uniform cross section and minimize carrier scattering at rough interface.[23] Accordingly, a quantitative understanding of the surface shape formation of 1D nanostructures is needed for the application of interest.

In this contribution we report the size-dependent morphological evolution of the 1D SnO_2 nanostructure growth using metal catalysts assistant thermal chemical vapor transport and condensation [vapor-liquid-solid (VLS) process]. In detail, we found that the shape formations of nanowires and nanobelts of SnO_2 are size dependent, i.e., the wire is favorable when the size is less than 90 nm and the belt is favorable when the size is more than 90 nm. For this issue, we proposed the nucleation thermodynamics, the growth kinetics, and the shape transition thermodynamics to elucidate our findings on the basis of the thermodynamic analysis at the nanometer scale.[24–29] Note that the size-dependent shape transformation from the initial stage of the nanowires nuclei to the nanobelts nuclei originates from the thermodynamic driving force of nucleation and growth of 1D nanostructures.

1D SnO_2 nanostructures including the nanowires and the nanobelts are grown on silicon substrates[30] using thermal chemical vapor transport and condensation with Au catalysts, and the detailed experiments and the characterization of morphologies and structures of the productions have been reported in the previous works.[30] Field emission scanning electron microscopy (FESEM), resolution transmission electron microscopy (HRTEM), and selected area electronic diffraction (SAD) are employed to identify the morphology and structure of 1D SnO_2 nanostructures. Figure 1(a) shows the morphology of typical 1D SnO_2 nanostructures. Interestingly, the FESEM statistic results definitely indicate that there are two kinds of 1D nanostructure, wire (b) and belt (c). In detail, the wire formation is favorable when the diameter of 1D nanostructures is less than 90 nm, and the belt formation is favorable when the diameter is more than 90 nm. Further, the size dependence of the shape of 1D SnO_2 nanostructures is shown in Fig. 1(d). Clearly, the optimal sizes of nanowires and nanobelts are 60 and 120 nm, respectively, the ratios of wires and belts in the prepared nanostructures are 63% and 37%, respectively, and a critical size of the shape transition from wire to belt is about 90 nm. Moreover, growth directions of nanowires and nanobelts are [200] and [211], respectively. We need to point out the reason that the [200] growth direction of the nanowires in this case is different from the $[00\bar{2}]$ growth direction of the nanowires

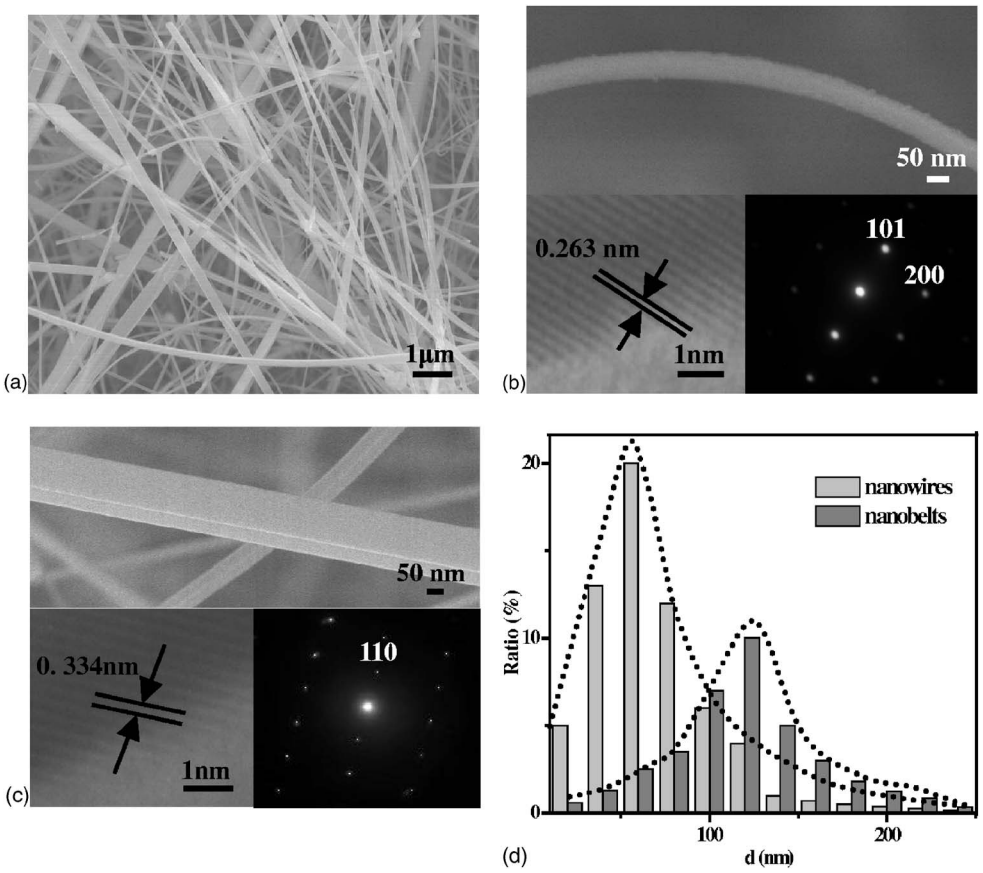

FIG. 1. (a) Low-magnifying FESEM image of SnO_2 nanowires and nanobelts. (b) High-magnifying FESEM image of a nanowire, in which a corresponding HRTEM image and SAD are shown below left right, respectively. (c) High-magnifying FESEM image of a nanobelt (the white line contrast on the nanobelt is another nanobelt whose wider plane of the cross-section inclines extremely towards left inside so as to seem thinner than the practical size), in which a corresponding HRTEM image and SAD are shown below left right, respectively. (d) The SEM statistics result of the radial size distribution of nanowires and nanobelts in the total prepared 1D nanostructures.

described in Ref. 30 is mainly due to the nanostructures not growing on the same substrate. In the case of Ref. 30, there are two substrates, i.e., substrates 1 and 2. On substrate 2, the growth direction of the nanowires is not only along $[00\bar{2}]$, and the [301] growth direction is also observed in the nanowires with little Sn nanocrystal or SnO_2 nanocrystal. Similarly, some nanobelts grow along the [301] direction, and some ones grow along the [211] direction on substrate 1.[30] Additionally, the SnO_2 nanoribbons can grow along the [110] direction or along the [203] direction,[31] and the ZnO nanobelts can grow along the [0001] direction or along the $[01\bar{1}0]$ direction.[32] Accordingly, these experimental results reveal that (i) the shape formation in the 1D SnO_2 nanostructure growth is size dependent; (ii) the optimal size of nanobelts is two times larger than that of nanowires; (iii) the ratios of wires and belts in the total synthesized nanostructures are 63% and 37%, respectively. Well known, 1D nanostructures grown by the VLS process are natural candidates.[23,33] However, there exists a fundamental issue: which physical and chemical mechanisms cause the size dependence of the shape formation during the 1D nanostructure growth by the VLS process. In the following section, we propose a series of theoretical analyses to pursue the issue on the basis of those observations above.

Nucleation thermodynamics. Generally, the Gibbs free energy is an adaptable measure of the energy of a state in phase transformation among competing phases. Thermodynamically, the phase transformation is promoted by the difference of the Gibbs free energies.[34] Therefore, we perform the nucleation of SnO_2 on the basis of the thermodynamic nucleation at the nanometer scale.[26,27] Considering the nanowire growth originates from the column-shape nuclei, and the formation of nuclei of the nanowire shown in Fig 1(b) is a process of the reaction precursors extracting from the saturated Au catalyst,[30] the Gibbs free energy difference of a column-shape nucleus is expressed

$$\Delta G_1 = -\Delta g_v \pi r_1^2 L_1 + \pi r_1^2(\delta_1 + \delta_1'') + 2\pi r_1 L_1 \delta_1, \qquad (1)$$

where δ_1 and δ_1'' are the nucleus-vapor and the nucleus-liquid interface energies, and the r_1 and L_1 are the radius and the height of the nucleus. The $\Delta g_v = -RT/V_m \ln(P/P_e)$ is the Gibbs free energy difference per unit volume, in which T, R, and V_m are the temperature, the gas constant, and the mole volume, and .P and P_e are the partial pressure of the Sn and the Sn vapor phase pressure in the thermal equilibrium coexistence with the liquid of composition in a flat surface. From Eq. (1), we deduce that the critical radius of r^*_1, the critical height of L^*_1, and the critical energy of ΔG^*_1 of

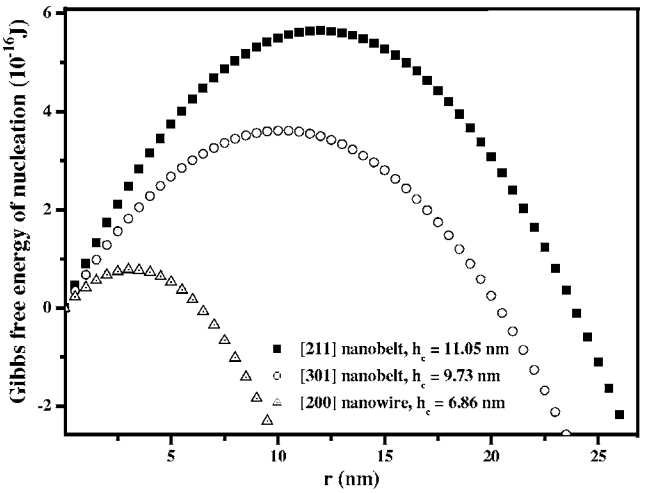

FIG. 2. The nucleation energies of a column-shape nucleus of nanowires and a rectangle-shape nucleus of nanobelts growing along the [211] and the [301] directions, respectively.

nuclei are $2\delta_1/\Delta g_v$, $2(\delta_1+\delta_1'')/\Delta g_v$, and $4\pi\delta_1^2(\delta_1+\delta_1'')/\Delta g_v^2$. Considering the nanobelt growth originates from the rectangle-shape nuclei. Note that, we use square-shape nuclei instead of rectangle-shape nuclei for simplifying the calculation in our case. Thus, the Gibbs free energy difference of a rectangle-shape nucleus is expressed

$$\Delta G_2 = -\Delta g_v r_2^2 L_2 + r_2^2(\delta_2 + \delta_2'') + 4r_2 L_2 \delta_2, \qquad (2)$$

where δ_2 and δ_2'' are the nucleus-vapor and nucleus-liquid interface energies, and the r_2 and L_2 are the side length and the height of the nucleus. Similarly, we have that the critical radius of r^*_2, the critical height of L^*_2, and the critical energy of ΔG^*_2 of nuclei are $4\delta_2/\Delta g_v$, $2(\delta_2+\delta_2'')/\Delta g_v$, and $16\delta_2^2(\delta_2+\delta_2'')/\Delta g_v^2$. Considering different growth directions of nanowires (the [200] direction) and nanobelts (the [211] or the [301] direction), Au catalyst, and the VLS nucleation mechanism,[27,28] δ_1 and δ_2 are 1.14 and 2.14 (or 1.82) J m^{-2},[35,36] δ_1'' and δ_2'' are 1.32 and 1.82 (or 1.66) J m^{-2},[27,37] T and V_m are 1223 K, and 16.24 cm^3/mole, and P and P_e are 3.29 and 1.047 Pa. Accordingly, r^*_1 and L^*_1 of nanowire nuclei are calculated to be 3.18 and 6.86 nm, r^*_2 and L^*_2 of nanobelt nuclei are calculated to be 11.94 (the [211] direction) or 10.18 nm (the [301] direction) and 11.05 (the [211] direction) or 9.73 nm (the [301] direction), and the size dependence of the nanowire and nanobelt nucleation is shown in Fig 2. Clearly, the radial size of the critical nucleus of nanobelts is approximately two times larger than the diameter of the critical nucleus of nanowires. Moreover, the nucleation energy of nanowire nuclei is lower than that of nanobelt nuclei that means that the nucleation probabilities of nanowires is higher than that of nanobelts, which are well consistent with our observations that the ratios of wires and belts in the total synthesized nanostructures are 63% and 37%, respectively.

Growth kinetics. Once the nucleation takes place, the increases in volume afforded by the continuous supply of the reaction precursors extracting from the saturated Au catalyst

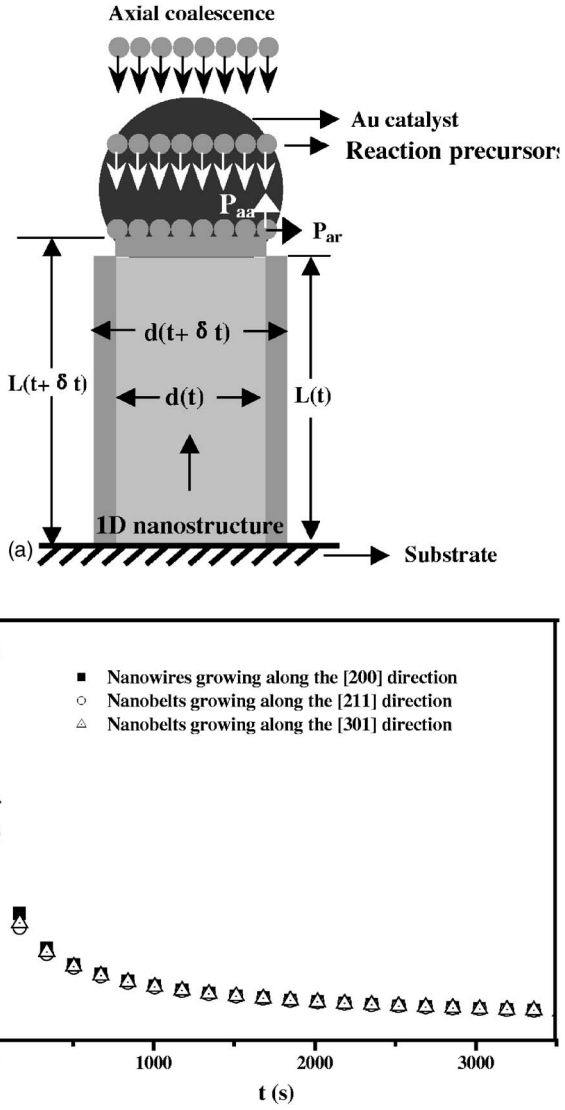

FIG. 3. (a) The growth mechanism sketch map of the 1D nanostructure (the radial cross section of the nanowire or nanobelt is shown here). (b) The growth rates of nanowire and nanobelt.

contributes to the increases in two feature sizes, radial size, and height, of nanowires and nanobelts on the basis of the VLS process.[27,28,38] The growth mechanism sketch map of the nanowire or the nanobelt is shown in Fig. 3(a). Thus, the radial growth rate of 1D nanostructures determines their final size. Well known, the surface free energy of nuclei and the concentration of the reaction precursors play key roles in the growth of nuclei,[39] in which the surface free energy is consisted of the surface energy[38,40,41] and the strain energy.[41,42] Meanwhile, the supply of the reaction precursors comes from the axial direction reaction precursors extracting from the saturated Au catalyst. The supply mechanism lead to the growth of the radius and height of 1D nanostructures, i.e., (i) axial supply resulting in an augment in the height (P_{aa}), (ii) axial supply resulting in an augment in the radius (P_{ar}) as follows:[41]

$$P_{ij} = \frac{\exp\left(-\frac{\Delta E_{ij}}{KT}\right)}{\sum_{i,j} \exp\left(-\frac{\Delta E_{ij}}{KT}\right)}, \quad \Delta E_{ij} = \Delta E_{Sij} + \Delta E_{Tij}, \quad i,j = a,r. \tag{3}$$

K is the Boltzman constant and T is the growth temperature. Thinking of the free energy ΔE_{ij} gaining in each case, we assume that the radial size of nanowires and nanobelts is large enough to make the surface energy ΔE_{Sij} much smaller than the strain energy ΔE_{Tij}. Thus, in each case, ΔE_{Tij} is written by:[41] $\Delta E_{Taa} = E_m(1-\sigma_m)\varepsilon_a^2$, $\Delta E_{Tar} = E_m \delta_m \varepsilon_a^2$, where E_m is the elastic modulus, δ_m is the Poisson's ratio of nanowires or nanobelts, and ε_a is the strain in the axial. Therefore, δt, the volume additivities of nanowires along the radial and axial are shown as follows:[41]

$$\frac{1}{4} L_1(t) d_1(t) \frac{\partial d_1(t)}{\partial t} = A \frac{1}{4} P_{ar} d_1(t)^2, \tag{4}$$

$$\frac{1}{4} d_1(t)^2 \frac{\partial L_1(t)}{\partial t} = 2A \frac{1}{4} P_{aa} d_1(t)^2. \tag{5}$$

Similarly, in the case of nanobelts, we have

$$\frac{1}{4} L_2(t) d_2(t) \frac{\partial d_2(t)}{\partial t} = A \frac{1}{4} P_{ar} d_2(t)^2, \tag{6}$$

$$\frac{1}{4} d_2(t)^2 \frac{\partial L_2(t)}{\partial t} = 2A \frac{1}{4} P_{aa} d_2(t)^2, \tag{7}$$

where $d_1(t)$ and $d_2(t)$ are the diameter (which is the function of the time t) of nanowires and the side length (which is the function of the time t) of nanobelts, $L_1(t)$ and $L_2(t)$ are the height (which is the function of the time t) of the nanowires and the nanobelts, A is the constant that is relative with the growth. In Eq. (4), the left section of the equation is the radial volume increase of the nanowire and the right section of the equation is the volume increase resulting from the axial supply precursors extracting from the Au catalyst, which leads to the augment of the radius of the nanowire. In Eq. (5), the left section of the equation is the axial volume increase of the nanowire and the right section of the equation is the volume increase resulting from the axial supply precursors extracting from the Au catalyst, which leads to the augment of the height of the nanowire. Meanwhile, in Eq. (6), the left section of the equation is the radial volume increase of the nanobelt and the right section of the equation is the volume increase resulting from the axial supply precursors extracting from the Au catalyst, which leads to the augment of the side length of the nanobelt. In Eq. (7), the left section of the equation is the axial volume increase of the nanobelt and the right section of the equation is the volume increase resulting from the axial supply precursors extracting from the Au catalyst, which leads to the augment of the height of the nanobelt. Neglecting the difference in strain energies in every type of growth, we attain approximate conclusions as follows:

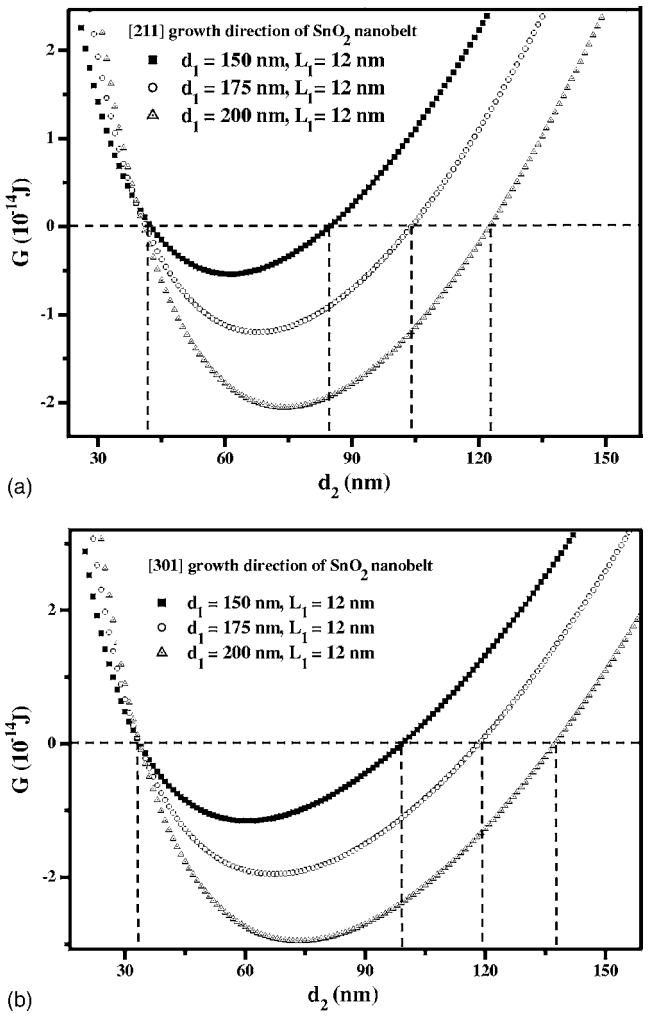

FIG. 4. Dependence of the Gibbs free energy of the shape transition during the initial stage of the nuclei growth. (a) The shape transition from the wire nuclei to the belt nuclei that grows along the [211] direction on the radial size of the nanowires nuclei under conditions of $d_1 = 150$, 175, and 200 nm, respectively, and $L_1 = 12$ nm. (b) The shape transition from the wire nuclei to the belt nuclei that growing along the [301] direction on the radial size of a nanowires nuclei under conditions of $d_1 = 150$, 175, and 200 nm, respectively, and $L_1 = 12$ nm.

$$d_1(t) \approx [2(t + 2r^*{}_1{}^2)]^{1/2}, \quad d_2(t) \approx \left[2\left(t + \frac{r^*{}_2{}^2}{2}\right)\right]^{1/2}, \tag{8}$$

where t is the growth time of nanostructures after nucleating, and $r^*{}_1$ and $r^*{}_2$ are critical sizes of nanowires and nanobelts. According to Eq. (8), the growth rates of nanowires and nanobelts are shown in Fig. 3(b). Distinctly, both growth rates of nanowire and nanobelt are basically the same during the growth of nanostructures. Therefore, the final size of nanobelts is approximately two times larger than that of nanowires, as $r^*{}_2$ is double that of $r^*{}_1$. This theoretical result is well in agreement with our findings shown in Fig. 1(d).

Shape transition thermodynamics. During the initial stage of the growth of nanowire nuclei, there are two probabilities of the shape transitions. One is from the wire nuclei to belt

nuclei with an increase to the volume of nanowire nuclei, and another one is from the belt nuclei to wire nuclei with and increase to the volume of nanobelt nuclei. In order to clarify which shape transition is preferable in thermodynamical, we need to compare the Gibbs free energies of wire and belt nuclei. Therefore, the Gibbs free energy of the shape transition, i.e., the Gibbs free energy difference between wire nuclei and belt nuclei, is given as $\Delta G = V\Delta P + \delta\Delta S$,[43] where ΔP is a pressure difference between nanowire nuclei and nanobelt nuclei, which is small enough to ignore. $V = \pi d_1^2 L_1/4 = d_2^2 L_2$ is the volume of nanowire nuclei and nanobelt nuclei, in which d_1 and L_1 are the diameter and height of nanowire nuclei, and d_2 and L_2 are the side length and height of the nanobelt nuclei, and $L_2 = \pi d_1^2 L_1/4d_2^2$. δ is the surface energy difference of the (200) plane of nanowire nuclei and the (211) plane of nanobelt nuclei. ΔS is the surface area difference between nanowires nuclei and nanobelt nuclei. Thus, ΔG can be expressed

$$\Delta G = \delta_2(4d_2L_2 + d_2^2) + \delta_2'' d_2^2 - \delta_1(\pi d_1 L_1 + \pi d_1^2/4) - \pi d_1^2 \delta_1''/4. \tag{9}$$

According to Eq. (9), when d_1 is equal to 150, 175, and 200 nm and $L_1 = 12$ nm, the relationships between ΔG and d_2 are shown in Fig. 4(a). Clearly, three curves intersect at the A point ($\Delta G = 0$ and $d_2 = 43$ nm), and $\Delta G < 0$ in these regions of AB, AC, and AD. In detail, in these regions, $\Delta G < 0$ means the Gibbs free energy of nanowire nuclei is larger than that of nanobelt nuclei, suggesting that the shape transition from wire nuclei to belt nuclei is probable. In instance, the nanowire nuclei with diameters of 150, 175, and 200 nm could transform into the nanobelt nuclei with radial sizes of 60, 70, and 80 nm, respectively. Note that, $\Delta G > 0$, when $d_1 < 120$ nm, implying that the shape transition from wire nuclei to belt nuclei of nanowire nuclei with the diameter less than 120 nm is not thermodynamically expected. When the nanobelts grow along the [301] direction, according to the Eq. (9), the relationships between ΔG and d_2 are shown in Fig. 4(b). Clearly, three curves intersect at the E point ($\Delta G = 0$ and $d_2 = 34$ nm), and $\Delta G < 0$ in these regions of EF, EG, and EH. The nanowire nuclei with diameters of 150, 175, and 200 nm could transform into the nanobelt nuclei with radial sizes of 60, 70, and 80 nm, respectively. Note that, $\Delta G > 0$, when $d_1 < 90$ nm, implying that the shape transition from the wire nuclei to the belt nuclei of nanowire nuclei with the diameter less than 90 nm is not thermodynamically expected. To sum up, the difference between the calculation results according to two different growth directions of the nanobelts is not so large that the conclusions are basically consistent and acceptable. Therefore, the larger nanowire nuclei sizes are, the easier the shape transition from wire nuclei to belt nuclei is, from the viewpoint of thermodynamic driving force. In fact, these theoretical predictions are not only consistent with experiments shown in Fig. 1(d), but also are physical origins of the experimental observations that both the wire formation with small size and the belt formation with large size are favorable during the growth of nanostructures.

In summary, we have systematically investigated the physical and chemical mechanisms of the shape evolution of 1D SnO_2 nanostructures in both experimental and theoretical. Based on experiments and theories, we found that the thermodynamic driving force, the Gibbs free energy difference between two phases, is always responsible for the shape choice in the different growth stages such as nucleation, growth, and structural transition of 1D nanostructures, implying that the thermodynamic driving force is one of the physical origins causing the interesting morphological transformation in the growth of 1D nanostructures. Meanwhile, our studies suggested that the revealed physical mechanisms could be expected to generally apply to control the shape of 1D nanostructures during the growth for purpose of fundamental researches and potential applications.

The National Natural Science Foundation of China (Contract No. 50525206), the Ministry of Education (106126) and the Natural Science Foundation of Guangdong (036596) funded this work.

*Corresponding author. Email address: stsygw@mail.sysu.edu.cn

[1] Y. Xia, P. Yang, Y. Sun, Y. Wu, B. Mayers, B. Gates, Y. Yin, F. Kim, and H. Yan, Adv. Mater. (Weinheim, Ger.) **15**, 353 (2003).
[2] S. Ferrere, A. Zaban, and B. A. Gsegg, J. Phys. Chem. B **101**, 4490 (1997).
[3] Y. S. He, J. C. Cambell, R. C. Murphy, M. F. Arendt, and J. S. Swinnea, J. Mater. Res. **8**, 3131 (1993).
[4] G. Ansari, P. Boroojerdian, S. Sainkar, R. N. Karekar, R. C. Alyer, and S. K. Kulkarni, Thin Solid Films **295**, 271 (1997).
[5] O. K. Varghese and L. K. Malhotra, Sens. Actuators B **53**, 19 (1998).
[6] X. F. Duan, Y. Huang, Y. Cui, J. Wang, and C. M. Leiber, Nature (London) **409**, 66 (2001).
[7] Z. Liu, D. Zhang, S. Han, C. Li, T. Tang, W. Jin, X. Liu, B. Lei, and C. Zhou, Adv. Mater. (Weinheim, Ger.) **15**, 1754 (2003).
[8] M. S. Arnold, Ph. Avouris, Z. W. Pan, and Z. L. Wang, J. Phys. Chem. B **107**, 659 (2003).
[9] L. L. Fields and J. P. Zheng, Appl. Phys. Lett. **88**, 263102 (2006).
[10] E. Comini *et al.*, Appl. Phys. Lett. **81**, 1869 (2002).
[11] Z. L. Wang, J. Phys.: Condens. Matter **16**, R829 (2004).
[12] R. V. Chamberlin, Nature (London) **408**, 337 (2000).
[13] P. Alivisato, Nano Lett. **1**, 109 (2001).
[14] R. V. Chamberlin, Phys. Lett. A **315**, 313 (2003).
[15] S. Abe and A. K. Rajagopal, Phys. Rev. Lett. **91**, 120601 (2003).
[16] Z. L. Wang, X. Y. Kong, and J. M. Zuo, Phys. Rev. Lett. **91**, 185502 (2003).
[17] C. X. Wang, Y. H. Yang, Q. X. Liu, and G. W. Yang, J. Phys. Chem. B **108**, 728 (2004).
[18] C. X. Wang, Y. H. Yang, N. S. Xu, and G. W. Yang, J. Am. Chem. Soc. **126**, 11303 (2004).
[19] Q. Li, K. W. Kwong, D. Ozkaya, and D. J. H. Cockayne, Phys. Rev. Lett. **92**, 186102 (2004).

[20] V. Garcia-Morales, J. Cervera, and J. Pellicer, Phys. Rev. E **67**, 062103 (2003).
[21] K. Pohl, M. C. Bartelt, J. de la Figuera, N. C. Bartelt, J. Hrbek, and R. Q. Hwang, Nature (London) **397**, 238 (1999).
[22] K. Thurmer, C. B. Carter, N. C. Bartelt, and R. Q. Hwang, Phys. Rev. Lett. **92**, 106101 (2004).
[23] F. M. Ross, J. Tersoff, and M. C. Reuter, Phys. Rev. Lett. **95**, 146104 (2005).
[24] C. Y. Zhang, C. X. Wang, Y. H. Yang, and G. W. Yang, J. Phys. Chem. B **108**, 2589 (2004).
[25] Q. X. Liu, C. X. Wang, and G. W. Yang, Phys. Rev. B **71**, 155422 (2005).
[26] Q. X. Liu, C. X. Wang, N. S. Xu, and G. W. Yang, Phys. Rev. B **72**, 085417 (2005).
[27] C. X. Wang, Q. X. Liu, N. S. Xu, and G. W. Yang, J. Phys. Chem. B **109**, 9966 (2005).
[28] C. X. Wang, J. Chen, G. W. Yang, and N. S. Xu, Angew. Chem., Int. Ed. **44**, 7414 (2005).
[29] C. X. Wang and G. W. Yang, Mater. Sci. Eng., R. **49**, 157 (2005).
[30] B. Wang, Y. H. Yang, C. X. Wang, and G. W. Yang, J. Appl. Phys. **98**, 073520 (2005).
[31] J. Q. Hu, X. L. Ma, N. G. Shang, Z. Y. Xie, N. B. Wong, C. S. Lee, and S. T. Lee, J. Phys. Chem. B **106**, 3823 (2002).
[32] Z. W. Pan, Z. R. Dai, and Z. L. Wang, Science **291**, 1947 (2001).
[33] R. S. Wagner and W. C. Ellis, Appl. Phys. Lett. **4**, 89 (1964).
[34] G. W. Yang and B. X. Liu, Phys. Rev. B **61**, 4500 (2000).
[35] J. Oviedo and M. J. Gillan, Surf. Sci. **463**, 93 (2000).
[36] B. Slater, C. R. Catlow, D. H. Gay, D. E. Williams, and V. Dusastre, J. Phys. Chem. B **103**, 10644 (1999).
[37] L. Vitos, A. V. Ruban, H. L. Skriver, and J. Kollar, Surf. Sci. **411**, 186 (1998).
[38] S. J. Kwon and J. G. Park, J. Chem. Phys. **122**, 214714 (2005).
[39] Q. X. Liu, C. X. Wang, Y. H. Yang, and G. W. Yang, Appl. Phys. Lett. **84**, 4568 (2005).
[40] F. Witt and R. W. Vook, J. Appl. Phys. **39**, 2773 (1968).
[41] S. J. Kwon, J. Phys. Chem. B **110**, 3876 (2006).
[42] J. Pelleg, L. Z. Zerin, and S. Lungo, Thin Solid Films **197**, 117 (1991).
[43] L. H. Liang, F. Liu, D. X. Shi, W. M. Liu, X. C. Xie, and H. J. Gao, Phys. Rev. B **72**, 035453 (2005).